Structural Engineering and Mechanics, Vol. 28, No. 6 (2008) 715-725
DOI: http://dx.doi.org/10.12989/sem.2008.28.6.715

Effect of design parameters on the anti-penetration properties of space armor

Tso-Liang Teng†

Department of Mechanical and automation Engineering, Da-Yeh University, 112 Shan-Jiau Rd., Dah-Tsuen, Chang-hua, Taiwan 515, R.O.C.

Ta-Ming Shih and Cheng-Chung Lu

Department of Weapon System Engineering, Chung Cheng Institute of Technology, National Defense University, Taiwan, R.O.C.

(Received October 13, 2006, Accepted January 28, 2008)

Abstract. New types of armor, including space armor, multiple-layered armor, composite armor and modular armor have been successfully developed and installed on the armored vehicles of several nations. The protective capability of armor against penetration is established. Of developed composite armor, space armor has a simple structure and is easy to produce and can be produced at low cost. This study uses the finite element package DYTRAN and the pre and post processor PNTRAN to elucidate the ballistic resistance and penetration of space armor. Factors such as armor thickness, space between armors and projectile profile are considered. A technique for simulating the protection afforded by armor and supporting the design of space armor is developed.

Keywords: Anti-penetration; space armor; DYTRAN.

1. Introduction

Since WWII, armored vehicles have been the most effective weapons for occupying territory because of their strong armor and large firepower. Recently, the designs of the protective armor structure and the ammunition have been greatly improved. The precision of ammunition rounds, and their ability to penetrate armor have been increased, and the capacity of armor to protect has also improved remarkably. Armor is usually improved by selecting better materials and implementing new rework processes. The earliest armor used mild steel. However, its protective capability is poor, and armor-piercing rounds from machine guns could easily penetrate the mild steel. New types of armor, including space armor, multiple-layered armor, composite armor and modular armor have been successfully developed and installed on the armored vehicles of several nations. The protective capability of armor against penetration is established. For example, space armor protects the turret of the German Leopard I A1, rubber layered armor steel plates are attached to the turret at a

† Professor, Corresponding author, E-mail: tlteng@mail.dyu.edu.tw

prescribed distance all around it, making the protection provided by the cast turret similar to the that of a type turret shaped by welding a homogeneous and rolled armor steel plate. Israel's Merkave main battle tank also has space armor structure. The fuel tank and engine of the Merkava are between the fore-armor plate and the crew cabinet spacer, markedly improving the safety of the crewmembers. Experiments have established that the protective capacity of 100 mm-thick fuel layers between two pieces of space armor is equivalent to that of a 25 mm-thick armor steel plate. However, the fuel tank of the Merkava main battle tank is 300 mm-thick, equivalent to 75 mm more front-armor. The specially designed fuel tank absorbs the energy of a round with which it is directly shot, without explosion, further reducing the power of the round, protecting the crewmembers even though the outer armor has been penetrated. The penetration of a projectile into a single-layered metal target has for a long time been an important area of study. However, studies of penetration to increase the ballistic resistance of composite armor are very few and have always been kept secret by leading military countries. Of developed composite armor, space armor has a simple structure and is easy to produce and can be produced at low cost. The penetration characteristics of space armor in terms of design parameters such as the target material, its thickness, inclination to the trajectory of the projectile, its distance from the target, its filling and even the profile of the shell are worthy of investigation.

Several researchers have studied the characteristic of space armor. Radian and Goldsmith (1988) used dull-nosed and sharp-nosed rounds with a diameter of 12.57 mm and a length of 38.1 mm in experiments to penetrate multi-layered targets. They demonstrated that the ballistic resistance of multi-layered targets of equal layer thickness and grid length is less than that of a single-layered target. Almohandes *et al.* (1996) used a 7.62 mm caliber bullet with an aspect ratio of 4.2 and different muzzle velocities to perform ballistic testing on space and composite armor filled with FRP. They found that, for a given total thickness, the total ballistic resistance is improved by reducing the number of steel plates or increasing the thickness of the rear plate. Yatteau *et al.* (1986) performed a series of ballistic tests and constructed an empirical residual mass formula for the penetration of a steel cube through the space armor. Naz (1987) combined numerical simulation and experimental results to determine the ballistic resistance and deformation of a multi-layered steel plate under the impact of a steel ball at various projecting velocities. Consequently, a semi-empirical relationship can be obtained between the deformation of the steel ball and its residual velocity. O'Donnell (1993) shot a 12.7 caliber tapered-headed steel projectile at ceramic and Kevlar multi-layer plates at an initial velocity of 800 m/s to confirm the deformation of the target plate, both analytically and experimentally. Chao and Chang (2000) applied energy density fracture theory and PEDDA software to evaluate the fracture conditions of aluminized and steel multi-layered plates penetrated by tapered sharp nosed steel bullets made of tungsten alloys. Chen (1989) utilized PRONTO 2D to simulate a double-layered concrete plate with a rock material model, hit by a tapered sharp-nosed bullet with a boost plate. The results of the simulation were very close to the test data, and a damage model was developed. Chin and Lim (1991) applied a VEC/DYNA 3D model to simulate the behavior of grid ceramic chips hit by the cylindrical tungsten alloys body. Liu and Shu (1999) employed DYNA 2D to analyze the penetration of a multi-layer target shot by a 2g steel ball. They determined that if the distance between the two layers exceeds the length of the projectile, then the ballistic resistance exceeds that of a single layer target plate with the same thickness. McGlaun (1994) studied the penetration of two-layered space armor by a bullet. The first layer and the second broke the projectile into small pieces, which were brought to rest. Yatteau and Dzwilewski (2003) proposed new target interaction and response models for partial impacts between

tumbling long rod penetrators and spaced plate targets. Chocron *et al.* (2003) presented a blended model to calculate the semi-infinite portion penetration using momentum balance method, and determined projectile perforation using the Ravid-Bodner failure modes. In addition, the model was extended to handle multiple plate impact. Robbins *et al*. (2004) used numerical method to study the effects of layer damage and an imperfect interface on load spreading and to gain insight into the underlying mechanisms governing the penetration resistance of layered targets.

Numerical simulations can take much less time than physical experiments and reduce development costs. This study uses the finite element package DYTRAN and the pre and post processor PNTRAN to elucidate the ballistic resistance and penetration of space armor. Factors such as armor thickness, space of armor and projectile profile are considered. A tool for simulating the protection afforded by armor and supporting the design of space armor is developed. The technique employed well-known and documented (Zukas 2004, Adenson 1987).

2. Verification

The experimental data concerning the collision between the steel plate and the ball in Liu and Shu (1999) are compared with the results of the finite element simulations herein, to demonstrate the application of the DYTRAN code in collision analysis.

2.1 Problem

A steel ball with a diameter of 8 mm collides perpendicularly with a steel plate with a thickness of 3 mm and a length and width of 62.88 mm at an initial velocity of 928 m/s, 852 m/s, 835 m/s, 717 m/s or 623 m/s. Tables 1 and 2 state the material properties of the ball and plate.

Table 1 The material properties of the steel ball

Mass density	7800 kg/m^3
Young's modulus	205 GPa
Poisson's ratio	0.3
Yield strength	635 MPa
Hardening modulus	2.05 GPa
Maximum plastic strain	2.0

Table 2 The material properties of the steel plate

Mass density	7800 kg/m^3
Young's modulus	205 GPa
Poisson's ratio	0.3
Yield strength	330 MPa
Hardening modulus	200 MPa
Maximum plastic strain	1.0

2.2 Model

In a double axially symmetric problem, the geometric profile of the ball and the plate can be represented using a quarter model. The steel ball is modeled by 700 8-node cubic elements and 858 nodes. The initial velocity, parallel to the Z axis, is given for the ball that collides with the steel plate. The plate is also modeled by 1536 8-node cubic elements and 2022 nodes. Both ball and plate materials are bilinear elastic-plastic materials. The erosion strain for the ball element is 2.0 and that for the plate is 1.0. Some of the ball elements erode during the penetration process, new contact surface continues to grow, so the boundary condition is assumed to be that all six faces of the cubic element are contact faces.

2.3 Results of analysis

Fig. 1 presents the velocity-time graph for the steel ball, penetrating the plate with an initial velocity of 928 m/s. At t = 14 μs, the velocity has become steady, with a residual velocity of 532.25 m/s, indicating that the ball has perforated penetrated the plate. Table 3 lists the simulated residual velocities given various initial velocities. The error between the results simulating using the Dytran finite element software and the experimental data are under 5% except when the initial velocity is 717 m/s (7.9%). These results establish the feasibility and reliability of the Dytran program, employed to analyze penetration and perforation.

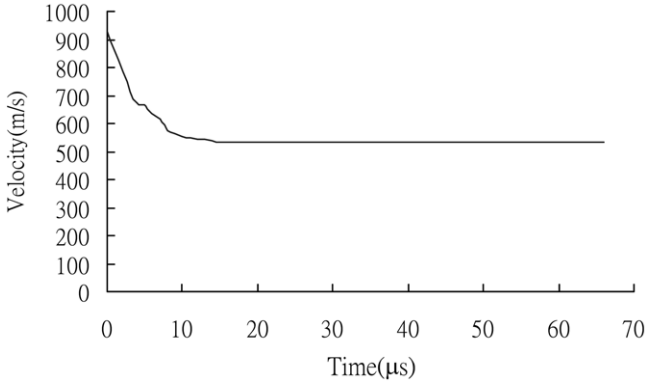

Fig. 1 The velocity-time graph for the steel ball

Table 3 The residual velocities with various initial velocities

Initial velocities (m/s) \ Residual velocities (m/s)	Experimental Liu and Shu (1999)	Dytran	Error (%)
928	531	532.25	0.2
852	459	468	2.0
835	431	450	4.4
717	300	323.7	7.9
623	163	163.67	0.4

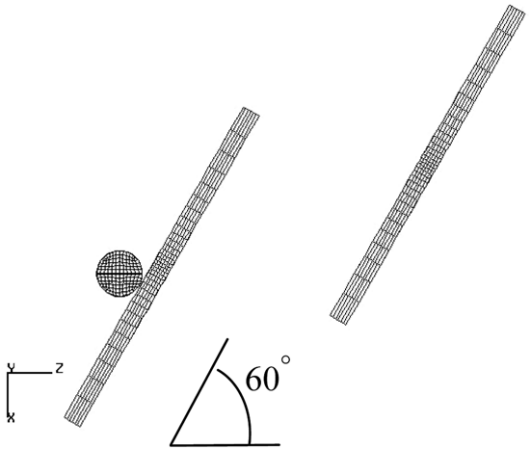

Fig. 2 A steel ball collides a double-layered space armor

3. The analysis of ballistic resistance for a double-layered space armor

3.1 Problem

The total thickness of the space armor is 6.35 mm. Each layer is assumed to be 3.175 mm in thick and 62.8 mm in length and width. The normal to the armor inclines 30 degrees with the projectile path, and the space between the two layers is 10 mm, as shown in Fig. 2. An 8 mm steel ball with an initial velocity 1300 m/s collides horizontally with the space armor.

3.2 Model

The problem can be modeled with one plane of symmetry. The boundary condition considered the armor plate with all edges fixed on. The steel ball is modeled by 1400 8-node cubic elements and 1829 nodes, all of which are given an initial velocity in the Z direction. Both layers are modeled by 3072 8-node cubic elements; 3927 nodes. Both ball and plate materials are bilinear elastic-plastic materials. The erosion strain for the ball element is 2.0 and for the plate is 1.0.

3.3 Results of analysis

Fig. 3 presents the deformation plot of the steel ball as it penetrates the space armor. The first layer is completely perforated and the steel ball is deformed. The steel ball rebounded from the second layer. The surface of the second layer has only a bowl-shaped contour, indicating that the steel ball was stopped. The figure thus shows the anti-penetration capacity of space armor. Fig. 4 plots the velocity of a steel ball, colliding with the double-layered space armor, against time, given an initial velocity 1300 m/s. The residual velocity component in the Z direction was reduced to 84.25 m/s. The motion of the ball is symmetric in the Y direction, so the associated speed is maximum as the ball strikes the armor and is thereafter around zero. The velocity component in the X direction is changed from 0 to –250.9 m/s, revealing the change in velocity in the - X direction after the steel ball collides with the inclined double-layered plate, The direction of motion of the

steel ball changes greatly upon collision with the second layer.

The improved capability of space armor is inferred to be related to the following causes.

(1) The penetration of the first layer will decelerate and deform the projectile and thus reduces the energy with which it collides with the second layer.

(2) The deviation of the direction of projectile from its original direction after perforating the first plate also increases the angle of incidence of the projectile with second plate, causing it to be rebounded after it has penetrated through the first layer.

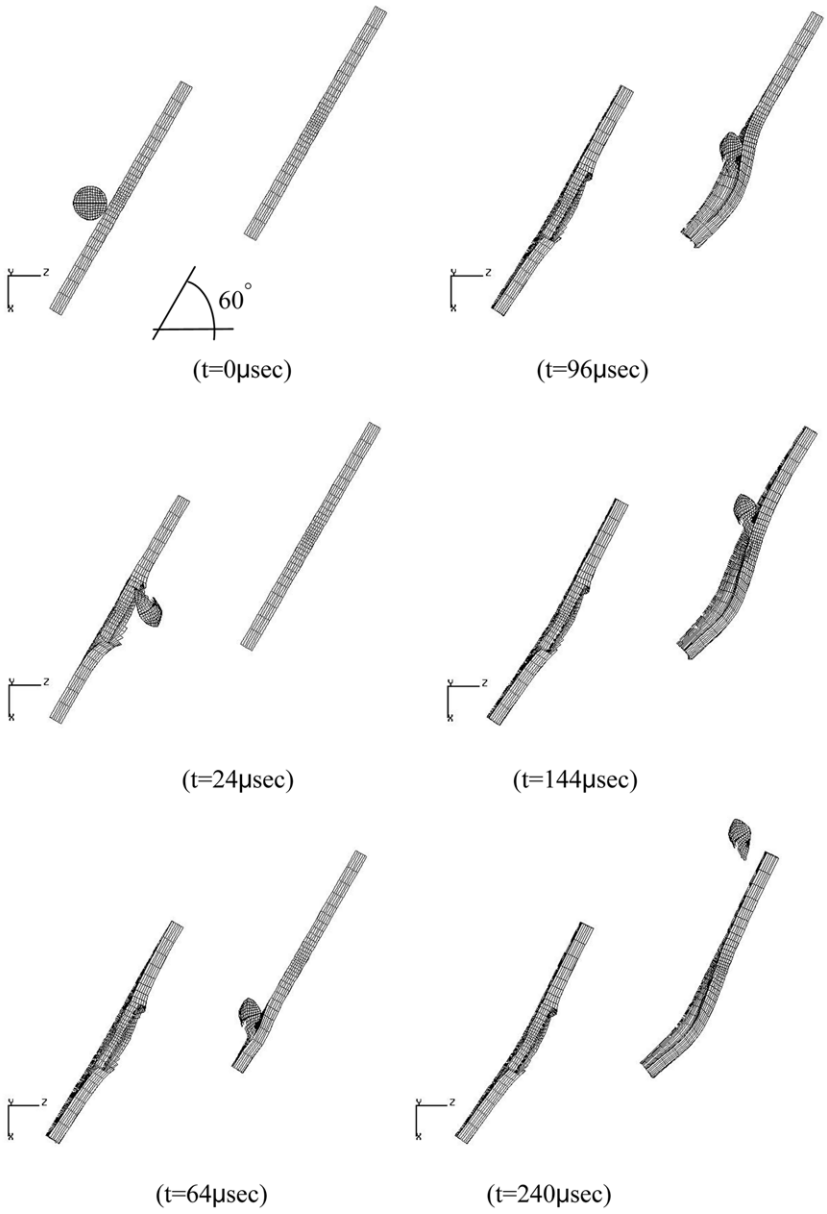

Fig. 3 The deformation plot of the steel ball and plate, V_{ball} = 1300 m/s ($t_1 = t_2 = 3.175$ mm, $d = 10$ mm)

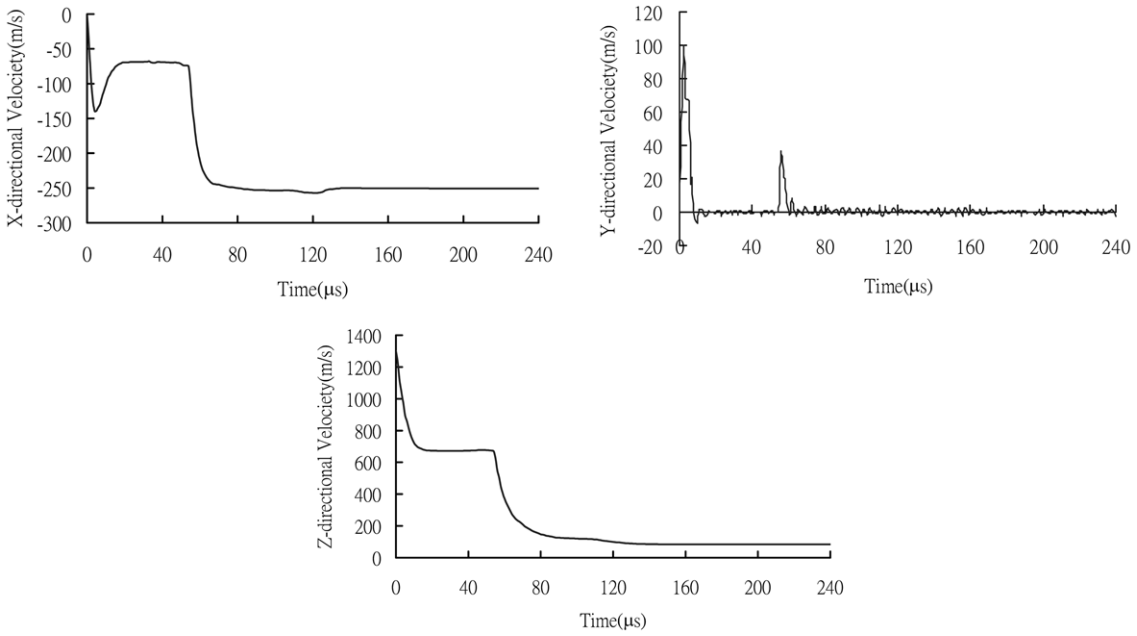

Fig. 4 The velocity-time of a steel ball collides space armor (t_1 = t_2 = 3.175 mm, d = 10 mm)

4. The analysis of space armor parameter

4.1 The gap width of space armor

Given armor with a total thickness of 6.35 mm and the same numerical resolution, the double-layered armor with a thickness of 3.175 mm and gap widths of 0.1 mm, 1 mm, 10 mm, 30 mm, 40 mm are separately considered. An 8 mm diameter projectile is assumed to collide with the armor in the normal direction with an initial velocity of 1300 m/s. Fig. 5 plots the residual velocity of the

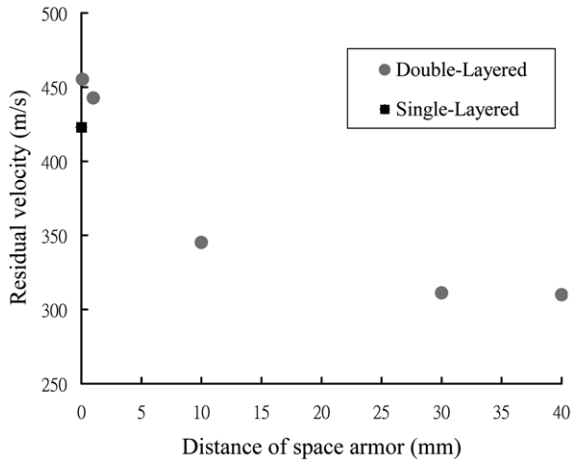

Fig. 5 The residual velocity of the steel ball with various distance of space armor (t_1 = t_2 = 3.175 mm)

steel ball after it has penetrated the space armor. The residual velocities at the four gap widths are 455.3 m/s, 442.7 m/s, 348.5 m/s, 311.42 m/s and 309.97 m/s separately. The plot implies that when the width of the gap between the two layers of the plate is 10 mm, 30 mm or 40 mm, the residual velocity is lower than that obtained using a single plate, implying that the ballistic resistance increase with the gap width. However, the residual velocity approaches a constant as the gap width increases over 30 mm, implying that this width only improves ballistic resistance over a certain range of values. At gap widths of 0.1 mm and 1 mm, the residual velocity is higher than that obtained using a single plate, and the ballistic resistance of double layers is less than that of a single layer, perhaps because the diameter of the steel ball is less that the width of the gap between the two layers.

4.2 The thickness of space armor

Again, a total thickness of 6.35 mm and the same resolution are considered. The fore-plate thickness, t_1, of the double-layered armor is 1.5875 mm and the rear plate thickness, t_2, is 4.7625 mm; the gap width is 30 mm. Fig. 6 plots the velocity of the steel ball, penetrating the armor, against time under the same initial conditions. The residual velocity of the projectile after it penetrates the first plate is 964.84 m/s and that after it penetrates the second plate is 296.86 m/s.

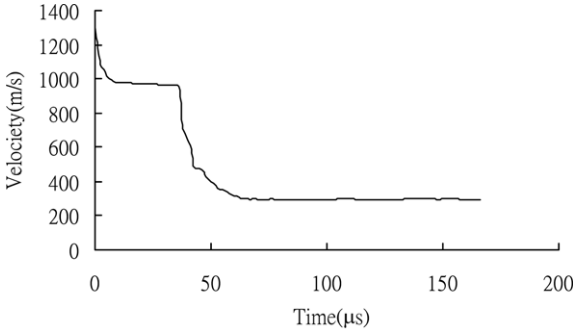

Fig. 6 The velocity-time of a steel ball collides space armor (t_1 = 1.5875, t_2 = 4.7625, d =10 mm)

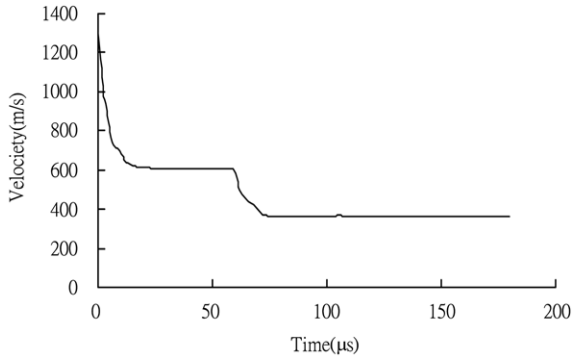

Fig. 7 The velocity-time of a steel ball collides space armor (t_1 = 4.7625, t_2 = 1.5875, d = 10 mm)

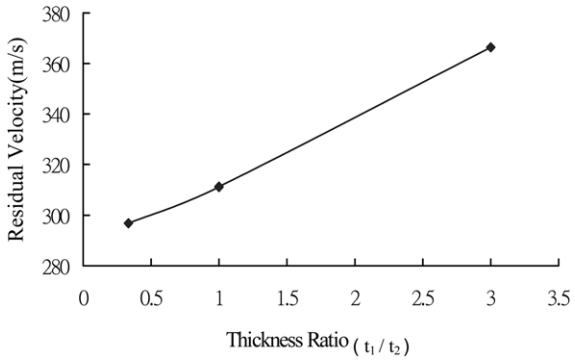

Fig. 8 The relationships between the residual velocity of projectile and the ratio of thicknesses of the two layers (t_1/t_2)

The fore and rear plates are then switched, yielding residual velocities of the projectile of 606.84 m/s after it penetrates the first plate and 366.39 m/s after it penetrates the second plate. Fig. 7 plots the residual velocity versus time. Using thinner plate as the fore plate yields better ballistic resistance than does using it as the rear plate.

Fig. 8 plots the relationships between the residual velocity of projectile and the ratio of thicknesses of the two layers (t_1/t_2). The magnitude of the residual velocity is proportional to the ratio of thicknesses. Therefore, in designing space armor, a smaller thickness ratio is preferred for a given gap width and weight of armor consideration.

4.3 The profile of projectile

Double-layered armor, with the same total thickness and numerical resolution as above is considered, under a direct collision with a cylindrical steel projectile of the same mass as used above; each layer is 3.175 mm thick and the width of the gap is 30 mm. The ratios of the length to the diameter (L/D) are 1, 6 and 15.

Fig. 9 plots the velocity of a cylindrical body (L/D = 1) after it penetrates the space armor. The

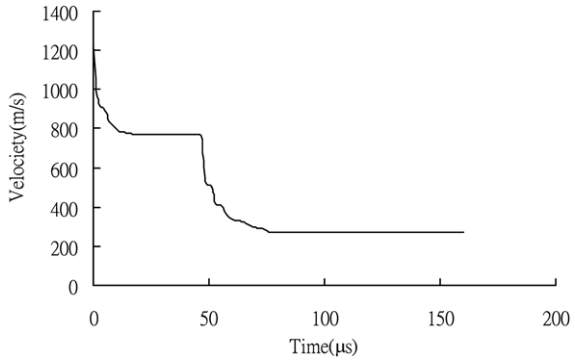

Fig. 9 The velocity-time of a cylindrical projectile collides space armor (t_1 = 3.175 mm, t_2 = 3.175 mm, d = 30 mm, L/D = 1)

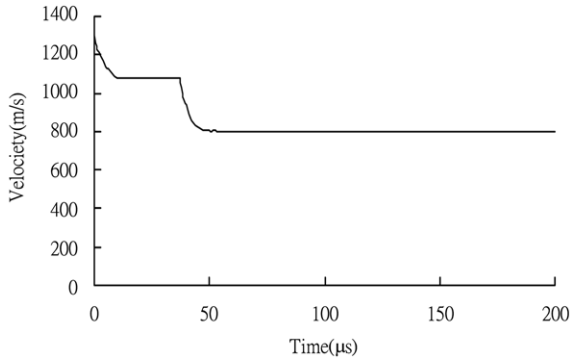

Fig. 10 The velocity-time of a cylindrical projectile collides space armor (t_1 = 3.175 mm, t_2 = 3.175 mm, d = 30 mm, L/D = 6)

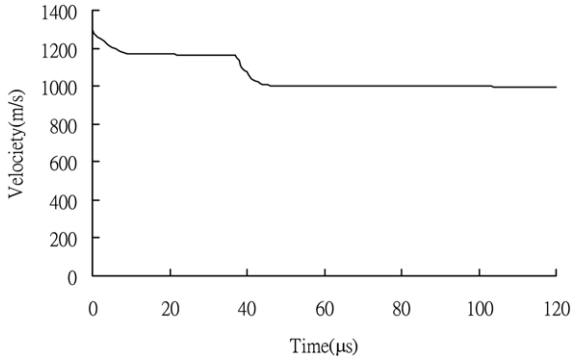

Fig. 11 The velocity-time of a cylindrical projectile collides space armor (t_1 = 3.175 mm, t_2 = 3.175 mm, d = 30 mm, L/D = 15)

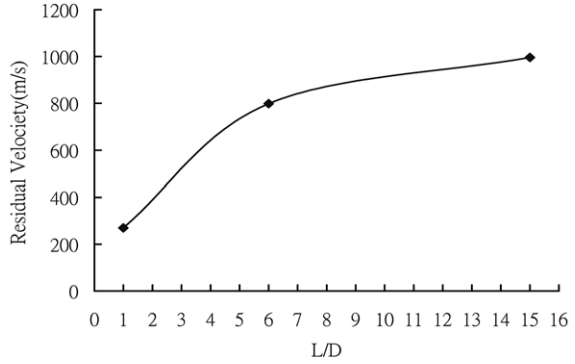

Fig. 12 The residual velocity of a cylindrical projectile versus the L/D ratio (t_1 = 3.175 mm, t_2 = 3.175 mm, d = 30 mm, L/D = 15)

residual velocity after it penetrates the fore plate is 772.5 m/s and that after it penetrates the rear plate is 269.67 m/s. Fig. 10 plots the velocity of a cylindrical body (L/D = 6) after it penetrates the space armor; the residual velocity after the fore plate is 1078.8 m/s and that after the rear plate is 798.97 m/s. Fig. 11 plots the velocity variation of a cylindrical body (L/D = 15) after it penetrates the space armor, the residual velocity after the fore plate is 1166.5 m/s and that the rear plate is 995.8 m/s. Fig. 12 plots the change in residual velocity versus the L/D ratio. In only the L/D = 1 case, the residual velocity is less than that of a steel ball projectile of the same mass, given the same gap width. In the other cases, the residual velocity exceeded that of the ball projectile, increasing with the L/D ratio. Results of any armor depend upon the projectile aspect ratio.

5. Conclusions

This study establishes a set of tools for analyzing the structure of spaced-plate armor and also elucidates the factors that dominate the protection afforded by space armor. Previous studies and this work support the following findings.

(1) For a steel plate with a given weight, increasing the gap width between the two layers increases the ballistic resistance of double-layered armor. However, once the gap exceeds a certain threshold, it not longer affects ballistic resistance.
(2) Given a particular same gap width and weight, double-layered space armor, a lower ratio of thickness of fore plate to thickness of rear plate yields better ballistic resistance.
(3) A more slender projectile more effectively pierces space armor. Space armor has poor ballistic resistance to slender projectiles as compared to compact projectiles.

References

Adenson, C.E. Jr. (1987), "An overview of the theory of hydrocodes", *Int. J. Impact Eng.*, **5**(1-4), 33-59.
Almohandes, A.A., Abdel-Kader, M.S. and Eleiche, A.M. (1996), "Experimental investigation of the ballistic resistance of steel-fiberglass reinforced polyester laminated plates", Composites, Part B 27B, 447-458.
Chao, C.K. and Chang, R.C. (2000), "Damage evaluation of two-layer targets impacted by a projectile", *Int. J. Impact Eng.*, **24**, 299-311.
Chen, E.P. (1989), "The application of numerical analysis on penetration mechanical engineering", *Conf. Penetration Mech. Eng.*, 2-1-2-49.
Chin, K.H. and Lim, S.E. (1991), "Simulation of projectile penetration into armor ceramics", ASME, AMD, **225**, 93-98.
Chocron, S., Anderson Jr C.E., Walker, J.D. and Ravid, M. (2003), "A unified model for long-rod penetration in multiple metallic plates", *Int. J. Impact Eng.*, **28**, 391-411.
Liu, C.K. and Shu, L.C. (1999), "The analysis on perforation resistance of multi-layered structure", The Conference of the Aeronautical and Astronautical Society/Explosive and Propellants Society of the Republic of China, 265-272.
McGlaun, M. (1994), "Overview of shock physics codes for analysis", Sandia National Laboratories Albuquerque, NM 87185-0819.
Naz, P. (1987), "Spaced plates penetration by spherical high-density fragments at high velocity", 10th Symp. Ballistics.
O'Donnell, R.G. (1993), "Deformation energy of kevlar backing plates for ceramic armors", *J. Mater. Sci. Letters*, **12**, 1485-1486.
Radin, J. and Goldsmith, W. (1988), "Normal projectile penetration of layered targets", *Int. J. Impact Eng.*, **7**,

229-259.
Robbins, J.R., Ding, J.L. and Gupta, Y.M. (2004), "Load spreading and penetration resistance of layered structures-a numerical study", *Int. J. Impact Eng.*, **30**, 593-615.
Yatteau, J.D. and Dzwilewski, P.T. (2003), "Adaptation of full impact penetration models to partial impact geometries for tumbling rods penetrating space plates", *Int. J. Impact Eng.*, **29**, 821-831.
Yatteau, J.D., Recht, R.F. and Dickinson, D.L. (1986), "High-speed penetration of spaced plates by compact fragments", 9th Symp. Ballistics.
Zukas, J.A. (2004), *Introduction to Hydrocodes* Elsevier Ltd.